British Journal of Pharmacology (2008) 155, 265–275

0007–1188/08 $32.00
www.brjpharmacol.org

RESEARCH PAPER

High-affinity blockade of voltage-operated skeletal muscle and neuronal sodium channels by halogenated propofol analogues

G Haeseler[1], M Karst[1], N Foadi[1], S Gudehus[1], A Roeder[1], H Hecker[2], R Dengler[3] and M Leuwer[4]

[1]*Department of Anesthesiology, Hannover Medical School, Hannover, Germany;* [2]*Department of Biometrics, Hannover Medical School, Hannover, Germany;* [3]*Department of Neurology and Clinical Neurophysiology, Hannover Medical School, Hannover, Germany and* [4]*Division of Clinical Sciences, The University of Liverpool, Liverpool, UK*

Background and purpose: Voltage-operated sodium channels constitute major target sites for local anaesthetic-like action. The clinical use of local anaesthetics is still limited by severe side effects, in particular, arrhythmias and convulsions. These side effects render the search for new local anaesthetics a matter of high interest.
Experimental approach: We have investigated the effects of three halogenated structural analogues of propofol on voltage-operated human skeletal muscle sodium channels ($Na_V1.4$) and the effect of one compound (4-chloropropofol) on neuronal sodium channels ($Na_V1.2$) heterologously expressed in human embryonic kidney cell line 293.
Key results: 4-Iodo-, 4-bromo- and 4-chloropropofol reversibly suppressed depolarization-induced whole-cell sodium inward currents with high potency. The IC_{50} for block of resting channels at −150 mV was 2.3, 3.9 and 11.3 μM in $Na_V1.4$, respectively, and 29.2 μM for 4-chloropropofol in $Na_V1.2$. Membrane depolarization inducing inactivation strongly increased the blocking potency of all compounds. Estimated affinities for the fast-inactivated channel state were 81 nM, 312 nM and 227 nM for 4-iodopropofol, 4-bromopropofol and 4-chloropropofol in $Na_V1.4$, and 450 nM for 4-chloropropofol in $Na_V1.2$. Recovery from fast inactivation was prolonged in the presence of drug leading to an accumulation of block during repetitive stimulation at high frequencies (100 Hz).
Conclusions and implications: Halogenated propofol analogues constitute a novel class of sodium channel-blocking drugs possessing almost 100-fold higher potency compared with the local anaesthetic and anti-arrhythmic drug lidocaine. Preferential drug binding to inactivated channel states suggests that halogenated propofol analogues might be especially effective in suppressing ectopic discharges in a variety of pathological conditions.
British Journal of Pharmacology (2008) **155,** 265–275; doi:10.1038/bjp.2008.255; published online 23 June 2008

Keywords: sodium channels; voltage-operated; local anaesthetics; propofol analogues

Abbreviations: ECI_{50}, half-maximum effect in inactivated channels; ECR_{50}, half-maximum effect on resting channels; *k*, Boltzmann parameter, slope factor of the availability curve; $Na_V1.2$, voltage-gated neuronal sodium channel (brain type IIA); $Na_V1.4$, voltage-gated skeletal muscle sodium channel; n_H, Hill coefficient; $V_{0.5}$, Boltzmann parameter, voltage of half-maximum channel availability; $\Delta V_{0.5}$, shift in the voltage dependence of channel availability

Introduction

Voltage-gated sodium channels are responsible for the increased sodium permeability during the rapid rising phase of the action potential. As mediators of membrane excitability, they represent important target sites for local anaesthetic, anti-epileptic and anti-arrhythmic drugs, which are known to block sodium channels in a voltage-dependent manner with higher affinity to inactivated conformations of the channel (Bean *et al.*, 1983; Balser *et al.*, 1996b; Vedantham and Cannon, 1999).

We have shown previously that the block of sodium channels by 2,6-dimethylphenol, a structural analogue of the aromatic alcohol and anaesthetic propofol on the one hand and the aromatic tail of lidocaine-like local anaesthetics on the other, mimics important features of sodium channel blockade by its parent compounds (Haeseler *et al.*, 2002). Recent molecular modelling studies involving several analogues of the local anaesthetic benzocaine have raised the hypothesis that the substituted benzene ring

Correspondence: Professor G Haeseler, Department of Anesthesiology; OE8050, Hannover Medical School, D- 30623 Hannover, Germany.
E-mail: Haeseler.Gertrud@MH-Hannover.de
Received 4 April 2008; revised 15 May 2008; accepted 22 May 2008; published online 23 June 2008

containing a functionally active group capable of binding a Na^+ ion (and thus mimicking the ammonium group of a charged local anaesthetic) constitutes the effective principle of local anaesthetic molecules because it determines their interaction with amino-acid residues critical for local anaesthetic binding in a hydrophobic cavity on the S6 segment of domain 4 in voltage-operated human skeletal muscle sodium channels ($Na_V1.4$) (Tikhonov *et al*., 2006; Godwin *et al*., 2005). Thus, it seems likely that phenol derivatives and benzocaine analogues act via a common local anaesthetic receptor site. Modelling the interaction of benzocaine analogues with their binding cavity has revealed that an increase in alkylation increases hydrophobic interactions and thus enhances the fit within the local anaesthetic binding cavity (Godwin *et al*., 2005). In accordance with these observations, we could show that an increase in C-chain length in the 2,6 positions of the phenolic hydroxyl group from methyl (2,6-dimethylphenol) (Haeseler *et al*., 2002) to isopropyl (propofol) (Haeseler *et al*., 2001b) and tertbutyl (2,6-di-*tert*-butylphenol) (Haeseler and Leuwer, 2003) groups increased blocking potency of the respective phenol derivative, although, in the case of 2,6-di-*tert*-butylphenol, the bulkier side chains almost prevented reversibility of block. Of all these phenol derivatives, the anaesthetic propofol was the most potent non-halogenated reversible blocker of sodium inward currents. Consequently, based on our previous observation that halogenation of an aliphatic phenolic blocker induces a strong increase in potency while retaining reversibility during washout (Haeseler *et al*., 2001a), we synthesized three halogenated structural analogues of propofol with the hypothesis that halogenated propofol analogues might constitute a novel class of highly potent sodium channel blockers. Preliminary results have shown that these structural analogues of propofol block sodium inward currents in rat ventricular myocytes with high potency (Bracken *et al*., 2006). The aim of this study was to characterize the interaction of 4-iodo-, 4-bromo- and 4-chloropropofol (Figure 1) with heterologously expressed $Na_V1.4$ and, additionally, the effect of one of the compounds (4-chloropropofol) on rat brain sodium channels ($Na_V1.2$) *in vitro*.

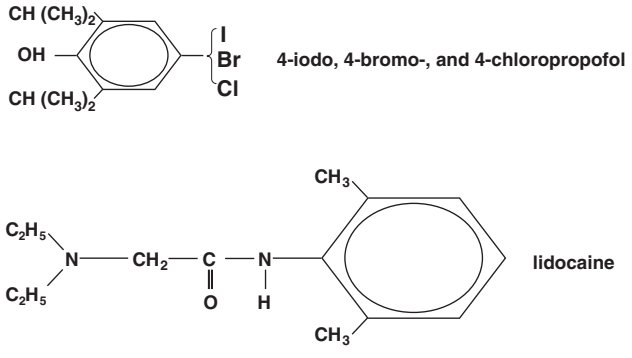

Figure 1 Structures of the halogenated propofol analogues used in this study (top) and, for comparison, the structure of lidocaine. The substituted benzene ring is a common feature of many local anaesthetic drugs.

Materials and methods

Transfection and cell culture

Stably transfected human embryonic kidney cell lines 293 expressing the α-subunit of either human skeletal muscle ($Na_V1.4$) or rat brain type IIA ($Na_V1.2$) sodium channels were a gift from Professor Lehmann–Horn (Ulm, Germany). Ion channel nomenclature conforms to the Guide to Receptors and Channels (Alexander *et al*., 2008). The expression vector pRc/CMV (Invitrogen, San Diego, CA, USA) was used for mammalian transfection (Mitrovic *et al*., 1994). Transfection was performed using calcium phosphate precipitation (Graham and Van der Eb, 1973). Permanent expression was achieved by selection for resistance to the aminoglycoside antibiotic geneticin G418 (Life Technology, Eggenstein, Germany) (Mitrovic *et al*., 1994). Successful channel expression was verified electrophysiologically. α-Subunits of skeletal muscle and neuronal sodium channels show normal gating characteristics (with respect to experiments in native tissue) when expressed in a mammalian cell line in the absence of the β-subunit (Chahine *et al*., 1994; Sarkar *et al*., 1995).

Solutions

4-Iodopropofol, 4-bromopropofol and 4-chloropropofol (for structures, see Figure 1) were synthesized by Braun Melsungen, Germany. The compounds were prepared as 1 M stock solution in ethanol and stored at −20 °C. The stock solution was dissolved directly in bath solution immediately before the experiments. Drug-containing vials were vigorously vortexed for 60 min. The solution was applied via a glass–polytetrafluoroethylene perfusion system and a stainless steel superfusion pipette. The bath solution contained [mM] NaCl 140, $MgCl_2$ 1.0, KCl 4.0, $CaCl_2$ 2.0, HEPES 5.0, dextrose 5.0. Patch electrodes contained [mM] $CsCl_2$ 130, $MgCl_2$ 2.0, EGTA 5.0, HEPES 10. All solutions were adjusted to 290 mosm L^{-1} by the addition of mannitol and to pH 7.4 by the addition of $Cs(OH)_2$. In the concentration range tested in this study, the diluent ethanol has no effect on sodium channels (Haeseler *et al*., 2001b).

Electrophysiology

Standard whole-cell voltage-clamp experiments (Hamill *et al*., 1981) were performed at 20 °C. Each experiment consisted of test recordings with the drug present at only one concentration, and of drug-free control recordings before and after the test. Each cell was exposed to one test concentration only. At least four independent experiments were performed at each concentration.

For data acquisition and further analysis, we used the EPC9 digitally controlled amplifier in combination with Pulse and Pulse Fit software (HEKA Electronics, Lambrecht, Germany). The EPC9 provides automatic subtraction of capacitive and leakage currents by means of a prepulse protocol. The data were filtered at 10 kHz and digitized at 20 μs per point. The input resistance of the patch pipettes was 2.0–3.5 MΩ and the capacitances of the cells were 9–15 pF; the residual series resistance (after 50% compensation) was 1.2–2.5 MΩ.

Experiments with a rise in series resistance were rejected. To minimize time-dependent shifts in the voltage dependence of steady-state inactivation (Wang *et al*., 1996), all test experiments were performed within 5 min of patch rupture. Under these experimental conditions, time-dependent hyperpolarizing shifts in control conditions were less than −2 mV (Haeseler *et al*., 2000).

Drug effects on the peak current amplitude were assessed at a holding potential close to the normal resting potential of muscle in physiological conditions (−70 mV) (Hodgkin and Horowicz, 1959), and at hyperpolarized membrane potentials (−150 and −100 mV). The residual sodium current (I/I_{max}) in the presence of drug (with respect to the current elicited with the same protocol in the respective control experiment) obtained with the different protocols was plotted against the applied concentration of the drug [*C*]. The averaged data were fitted using the Hill equation (Equation 1) yielding the concentration for half-maximum channel blockade (IC_{50}) and the Hill coefficient n_H.

$$\frac{I}{I_{max}} = \frac{IC_{50}^{n_H}}{IC_{50}^{n_H} + C^{n_H}} \quad (1)$$

The voltage dependence of the block and the affinity for depolarized channel states was further assessed by applying a double-pulse protocol. Currents elicited by test pulses (I_{test}), starting from varying prepulse potentials (from −150 to −5 mV), normalized to the current elicited at the most hyperpolarized prepotential (−150 mV), represent the relative fraction of channels that have not been inactivated during the 100 ms inactivating prepulse. Boltzmann fits to the resulting current–voltage plots yield the membrane potential at half-maximum channel availability ($V_{0.5}$) and the slope factor *k*, reflecting the 'voltage sensitivity' of inactivation gating (see Equation 2).

$$\frac{I}{I_{max}} = \frac{1}{1 + e^{\frac{v_{test} - V_{0.5}}{k}}} \quad (2)$$

In control conditions, the parameters of the Boltzmann fits reflect the voltage-dependence of the distribution between resting and fast-inactivated channels (the availability curve). In the presence of drug, the steady-state availability curve reflects drug association with rested and fast-inactivated channels. The conformational change induced by channel inactivation may increase the binding affinity for a sodium channel-blocking agent—the modulated receptor model for local anaesthetic action (Hille, 1992). Drug binding to inactivated channels is hardly accessible to a direct experimental approach, because inactivated channel states and all drug-bound channel states are unavailable on depolarization. A model-dependent method is generally applied to determine the affinity to fast-inactivated channel states. Tighter binding of the drug to fast-inactivated channels compared with resting channels—a typical feature of sodium channel blockade by lidocaine-like local anaesthetics—increases the fraction of unavailable channels at depolarized membrane potentials by more than just the sum of channel inactivation at a given membrane potential and block of the remaining resting channels at the respective membrane potential (Hille, 1992). This membrane-potential-dependent increase in the fraction of unavailable channels is revealed by a negative voltage shift $\Delta V_{0.5}$ in the channel availability curve that shows concentration dependence. The model-dependent assessment of the affinity to fast-inactivated channels is based on this concentration-dependence of the shift in the availability curve (Bean *et al*., 1983; Leuwer *et al*., 2004). The underlying assumption is that the higher amount of channel blockade achieved with consecutive membrane depolarization is determined by the distribution of channels between resting and fast-inactivated states along the voltage axis (that is, the channel availability curve) and by the different binding affinities of the blocking drug for the two channel states. The voltage shift $\Delta V_{0.5}$ in the presence of a drug would depend upon the drug concentration [*C*], according to Equation 3 (Leuwer *et al*., 2004). A fit of the model to $\Delta V_{0.5}$ plotted against concentration yields estimates for the concentration for half-maximum effect on fast-inactivated channels ECI_{50} and the Hill-type coefficient for drug binding to inactivated channels n:

$$\Delta V_{0.5} = k.\ln\left[\left(1 + \frac{[C]}{ECR_{50}}\right) / \left(1 + \frac{[C]^n}{ECI_{50}^n}\right)\right] \quad (3)$$

K and ECR_{50} are entered as constant factors. *K* is the slope factor of the availability curve in the controls and ECR_{50} is the concentration for half-maximum effect on resting channels, obtained at −150 mV holding potential.

After inactivation, channel reopening is impossible until the channels recover from inactivation, a process that requires several ms after membrane repolarization. Further information about drug effects on the kinetics of drug dissociation from the fast-inactivated state can be derived from the rate at which the channels recover from inactivation in the presence of the drug and from the accumulation of block during trains of repetitive pulses (use-dependent block). The time of membrane repolarization required to remove fast inactivation was assessed at −100 mV by a two-pulse protocol, with varying time intervals (up to 100 ms) between the inactivating prepulse and the test pulse. The time constants of recovery, τ_{rec}, were derived from biexponential fits to the fractional current after recovery from inactivation, plotted against the time interval between the inactivating prepulse and the test pulse (Equation 4).

$$I(t) = a0 + a1 \cdot e^{\frac{-t}{\tau 1}} + a2 \cdot e^{\frac{-t}{\tau 2}} \quad (4)$$

Use-dependent block was assessed at −150, −100 and −70 mV holding potential using trains of 10 ms pulses applied at 10 Hz and at −100 mV using 5 ms pulses of 50 and 100 Hz.

Statistical analysis

Statistical analysis was performed to reveal a potential difference in potency between the compounds in $Na_{V1.4}$ at a hyperpolarized holding potential (−150 mV). Curve fitting and parameter estimation of the Hill curves were performed using the program 'PROC NLMIXED' of SAS Release 8.02. In this model, the 'experiment' is treated as the subject variable and the parameter values (IC_{50} and n_H) are treated as normally distributed random factors. The mean differences of these

parameters between the three compounds were entered into the common model as fixed shift parameters ΔIC_{50} and Δn_H, activated for all data of the second data set. The corresponding (asymptotic) *t*-value was used to test the null hypothesis of no parameter difference against the two-sided alternative. The null hypothesis was rejected at $P<0.05$.

Results

Resting state affinity

We studied a total of 243 cells. Average currents in the control experiments following depolarization from −150 mV to 0 mV were -2.8 ± 1.2 nA in $Na_V1.4$ ($n=102$) and 2.5 ± 1.3 nA in $Na_V1.2$ ($n=77$). Maximum inward currents elicited by 10 ms pulses from either −150, −100 or −70 mV to 0 mV were suppressed by all compounds in the low μM range. A steady state of sodium channel blockade at a given concentration was reached during 60 s of drug application; however, recovery of sodium inward current during washout was incomplete. Peak inward currents following drug application in concentrations higher than the respective EC_{50} for block reached 70–80% of the control values during the 3–5 min washout period.

Residual sodium inward currents (with respect to control) in the presence of drug derived from at least five different experiments for each drug concentration were averaged to establish concentration–response plots. Hill fits to the averaged data yielded an IC_{50} value of 0.8, 2.5 and 6.9 μM at −100 mV holding potential for 4-iodopropofol, 4-bromopropofol and 4-chloropropofol in $Na_V1.4$, respectively, and of 22.0 μM for 4-chloropropofol in $Na_V1.2$. The amount of block achieved depended on the holding potential from which the depolarization was started. The respective IC_{50} values were reduced to 0.2, 1.0 and 1.4 μM ($Na_V1.4$) and 5.5 μM (4-chloropropofol in $Na_V1.2$) at −70 mV holding potential. At a strongly hyperpolarized potential (−150 mV; Figure 2) where all channels are in the resting state, the respective IC_{50} values were 2.3, 3.9 and 11.3 μM ($Na_V1.4$) and 29.2 (4-chloropropofol in $Na_V1.2$). 4-Chloropropofol was significantly less potent at −150 mV than 4-iodopropofol ($P=0.0008$) and 4-bromopropofol ($P=0.0058$); the difference between 4-iodopropofol and 4-bromopropofol did not reach statistical significance ($P=0.076$). Calculated values for the Hill coefficients n_H ranged between 0.7 and 1.0; no significant differences in Hill coefficients were detected between the compounds.

Inactivated state affinity

The increase in blocking potency at a holding potential of −70 mV, at which a fraction of the channels is inactivated, compared with −150 mV, at which all channels are expected to be in the resting state, suggests that the amount of block achieved by all compounds depends on the membrane potential and increases as the proportion of inactivated channels increases with respect to resting channels.

The increase in blocking potency achieved with consecutive membrane depolarization was further assessed using a double pulse protocol with 100 ms prepulses to depolarized membrane potentials before the test pulse (see Materials and methods section; Figures 3 and 4). In control conditions, half of the channels were unavailable at -65.8 ± 5.9 mV ($Na_V1.4$) and -51.6 ± 5.0 mV ($Na_V1.2$) because of fast inactivation.

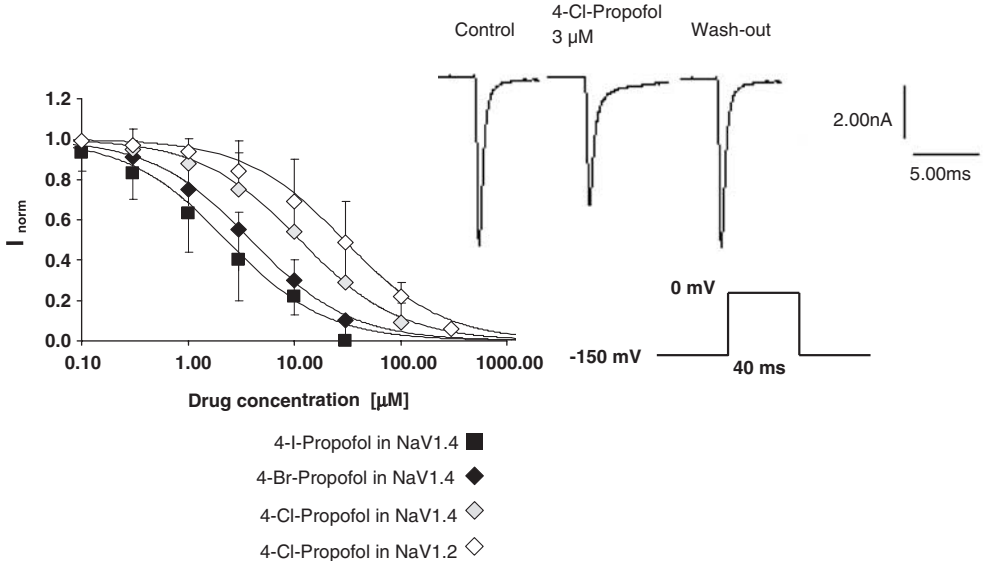

Figure 2 Block of resting channels at −150 mV holding potential. Left: concentration dependence of block of sodium inward current by 4-iodo-, 4-bromo- and 4-chloropropofol in $Na_V1.4$ and 4-chloropropofol in $Na_V1.2$ at −150 mV holding potential. Each symbol represents the mean value of the residual sodium currents in the presence of drug (I_{norm}, mean ± s.d.), derived from at least five independent experiments for each concentration tested. The solid lines are Hill fits to the averaged data yielding a half-maximum blocking concentration EC_{50}, of 2.3 μM for 4-iodopropofol, 3.9 μM for 4-bromopropofol and 11.3 μM for 4-chloropropofol in $Na_V1.4$, and 29.2 μM for 4-chloropropofol in $Na_V1.2$, respectively. Right: representative current traces following a 40 ms depolarization from −150 to 0 mV in the absence (control and washout) and presence of 3 μM 4-chloropropofol in $Na_V1.2$.

The slope factor k was 7.2 ± 1.0 ($Na_V1.4$) and 7.1 ± 0.6 ($Na_V1.2$). With exposure to all compounds, $V_{0.5}$ was shifted in the direction of more negative prepulse potentials; the degree of alteration showed concentration dependence. Estimates for the ECI_{50} derived from a fit of Equation 3 to the concentration dependence of the voltage shift for 4-iodo-, 4-bromo- and 4-chloropropofol in $Na_V1.4$, and 450 nM for 4-chloropropofol in $Na_V1.2$, as shown in the corresponding graphs in Figure 4, were 81, 310 and 227 nM, respectively (see Figure 4).

Time course of recovery from inactivated channel block

The time of membrane repolarization required to remove fast inactivation was assessed at −100 mV by a two-pulse protocol, with varying time intervals (up to 100 ms) between the inactivating prepulse and the test pulse. The time constants of recovery, τ_{rec}, were derived from biexponential fits to the fractional current after recovery from inactivation, plotted against the time interval between the inactivating prepulse and the test pulse (Equation 4).

In the absence of the drug, recovery time constants τ_{rec1} obtained for the neuronal and the skeletal muscle isoform were 3.4 ± 1.2 and 2.5 ± 0.5 ms, respectively. In the presence of drug, we found a slow component τ_{rec2} of 20–40 ms in both channel isoforms, which comprised 9, 21 and 49% of the current amplitude in 3 μM concentrations of 4-chloro-, 4-bromo- and 4-iodopropofol, respectively, in the skeletal muscle isoform and 1 and 10% of the current amplitude in 3 and 10 μM 4-chloropropofol in the neuronal isoform (Figures 5a and b). The fast time constants τ_{rec1} were increased to 6.2 ± 1.0 ms in 3 and 10 μM 4-chloropropofol in the neuronal isoform and to 4.6 ± 1.3, 5.7 ± 1.5 and 15.8 ± 7 ms in 3 μM concentrations of 4-chloro-, 4-bromo- and 4-jodopropofol, respectively, in the skeletal muscle isoform. This means that recovery from inactivated channel block at a hyperpolarized holding potential (−100 mV) should be too fast to accumulate frequency-dependent block at a stimulating frequency lower than 10 Hz.

The accumulation of block during trains of depolarizing pulses suggests that the interval between pulses is too short to allow recovery of sodium channel availability. Frequency-dependent block was defined as the additional reduction in sodium current for the last pulse relative to the first pulse in a test train in the presence of drug. At −100 mV, frequency-dependent block during 10 Hz trains was <5% for all compounds at concentrations below the IC_{50} for block of resting channels. However, during 100 Hz trains at −100 mV, the additional fall relative to the first pulse was 27, 13 and 9% in the presence of 30, 10 and 3 μM 4-chloropropofol in

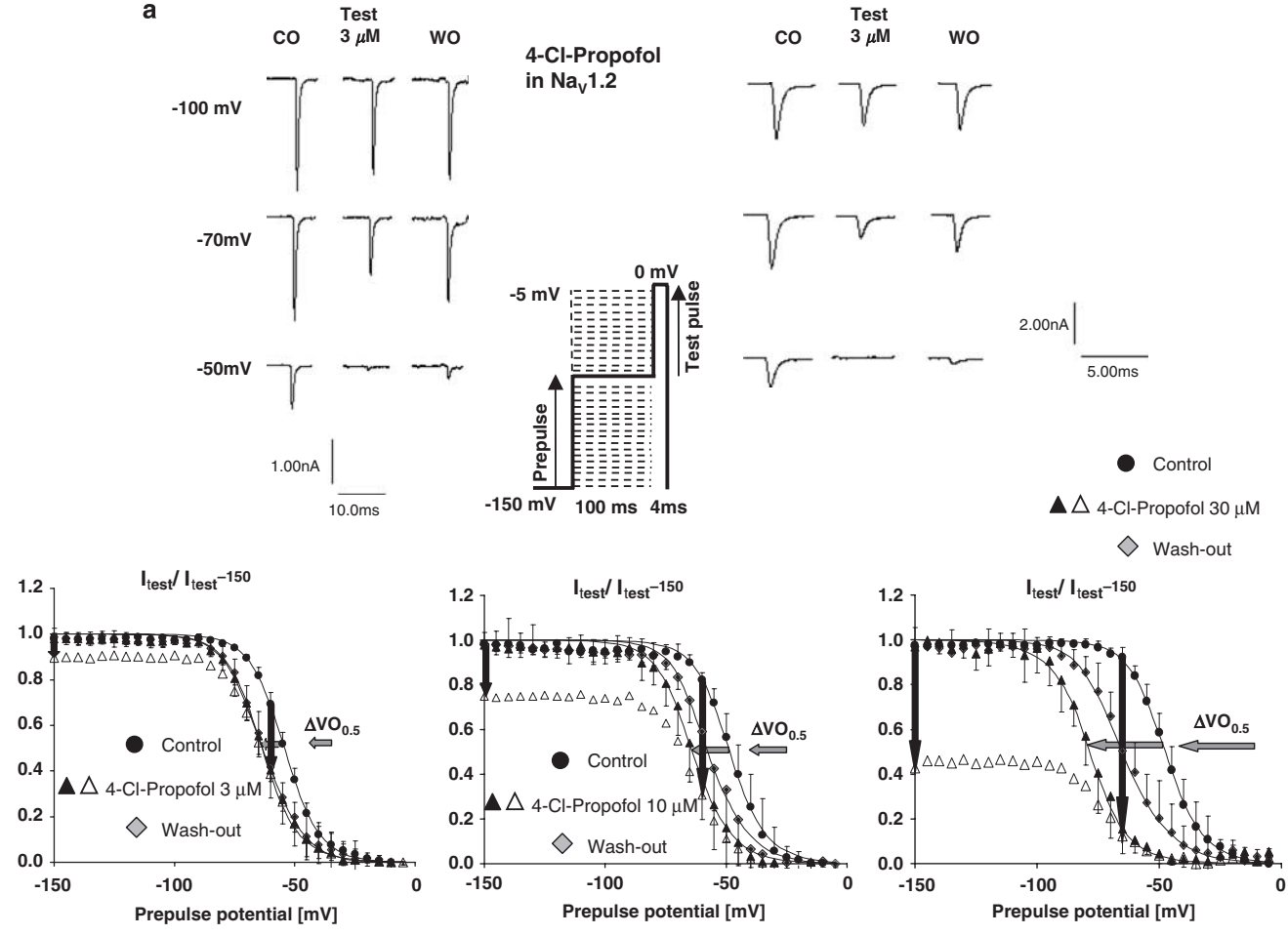

Figure 3 Continued.

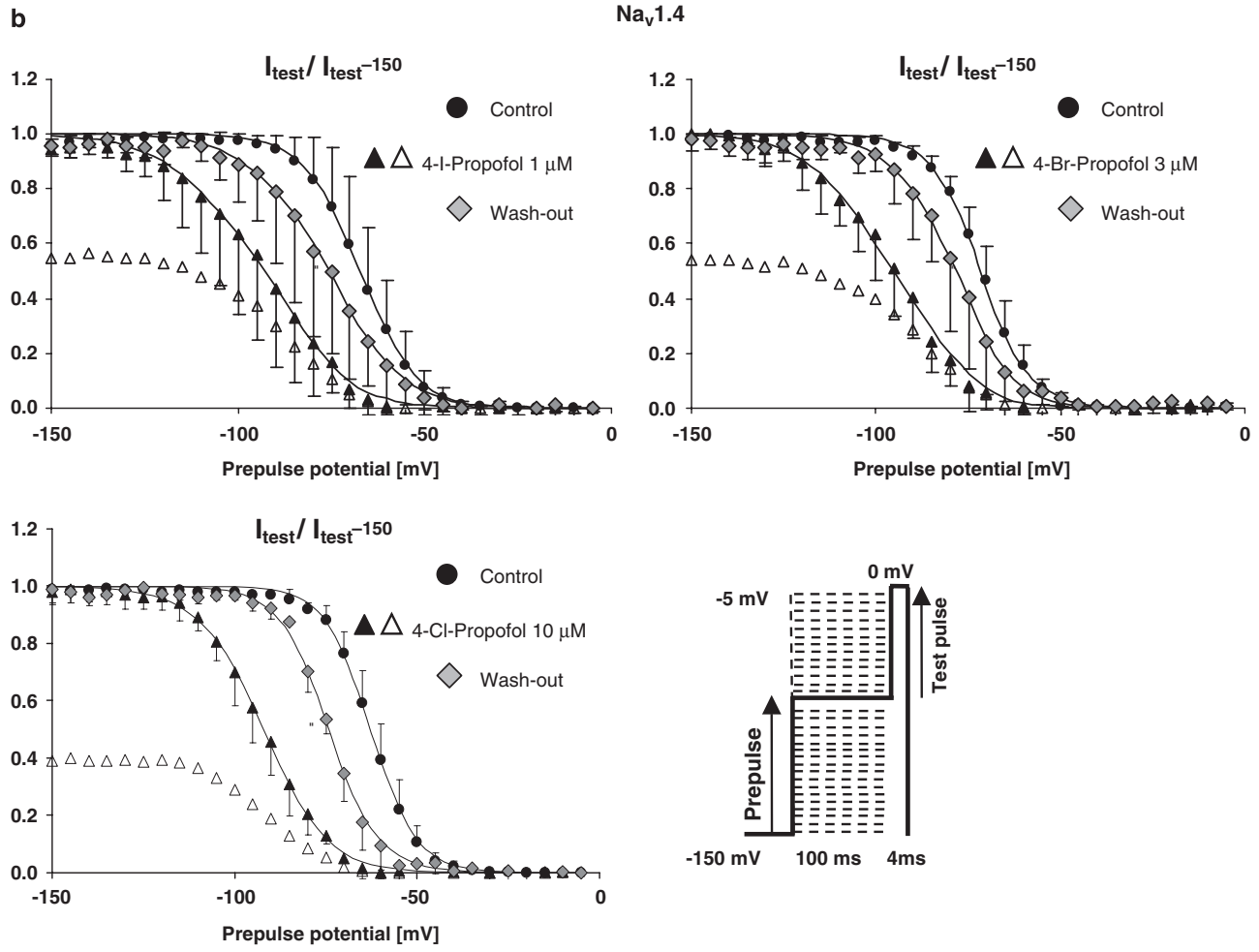

Figure 3 Affinity of 4-iodo-, 4-bromo and 4-chloropropofol to fast-inactivated channels derived from the concentration dependence of the shifts in the voltage-dependence of channel availability. (**a**) Top: representative current traces illustrating the increase in blocking potency of 3 μM (left) and 10 μM (right) 4-chloropropofol in $Na_V1.2$ neuronal sodium channels when depolarizations were started from more positive holding potentials—note that the current inhibition is complete at a potential near the potential for half-maximum channel inactivation (−50 mV) in control conditions. Bottom: steady-state availability curves assessed by a two-pulse protocol in the absence (control and washout) and presence of (from left to right) 3, 10 and 30 μM 4-chloropropofol in $Na_V1.2$ sodium channels. Each symbol represents the mean fractional current derived from seven different experiments, elicited by a 4 ms test pulse to 0 mV, following a 100 ms inactivating prepulse from −150 mV to the indicated prepulse potential. Currents were normalized to maximum value (in each series at −150 mV pre-potential); solid lines represent the best Boltzmann fit (Equation 2, Materials and methods section) to the data. The indicated errors are standard deviations. In the presence of drug, currents were normalized either to maximum value in the presence of drug (filled symbols) or to maximum value in the controls (empty symbols). Vertical arrows illustrate the increase in peak current suppression induced by the test drug at more depolarized potentials compared with −150 mV prepulse potential. This increase in the peak current suppression induced by the test drug at more depolarized prepulse potentials results in a voltage shift in the midpoints of the availability curve ($\Delta V_{0.5}$) illustrated by the vertical arrows. This voltage shift is concentration dependent; the concentration dependence of this effect is depicted in Figure 4. (**b**) The effects of 1 μM 4-iodopropofol, 3 μM 4-bromopropofol or 10 μM 4-chloropropofol on steady-state availability curves in $Na_V1.4$ sodium channels, assessed by a similar two-pulse protocol. Membrane depolarization increases blocking potency in all compounds, revealed by a voltage shift of the respective availability curve in the direction of negative pre-potentials.

the neuronal isoform, and 29, 17 and 11% in the presence of 1 μM 4-iodopropofol and 3 μM 4-bromo- and 4-chloropropofol, respectively, in the skeletal muscle isoform.

Discussion

The main result of this study is that, in line with our hypothesis, the insertion of a halogen in the para-position to the phenolic hydroxyl group of the propofol molecule yields compounds with very high potency to block voltage-operated sodium channels in a local-anaesthetic-like manner. The *in vitro* potency of halogenated propofols to block sodium channels is much higher than that of any local anaesthetic in clinical use at the present time, for example, almost 100-fold higher when compared with the local anaesthetic lidocaine (Fan *et al*., 1996), and about 20-fold higher when compared with the parent compound propofol (Haeseler *et al*., 2001b). The IC_{50} for block of skeletal muscle sodium channels in the resting state reported for lidocaine is 460 μM (Fan *et al*., 1996; Leuwer *et al*., 2004). Our study shows that halogenated propofol analogues block skeletal

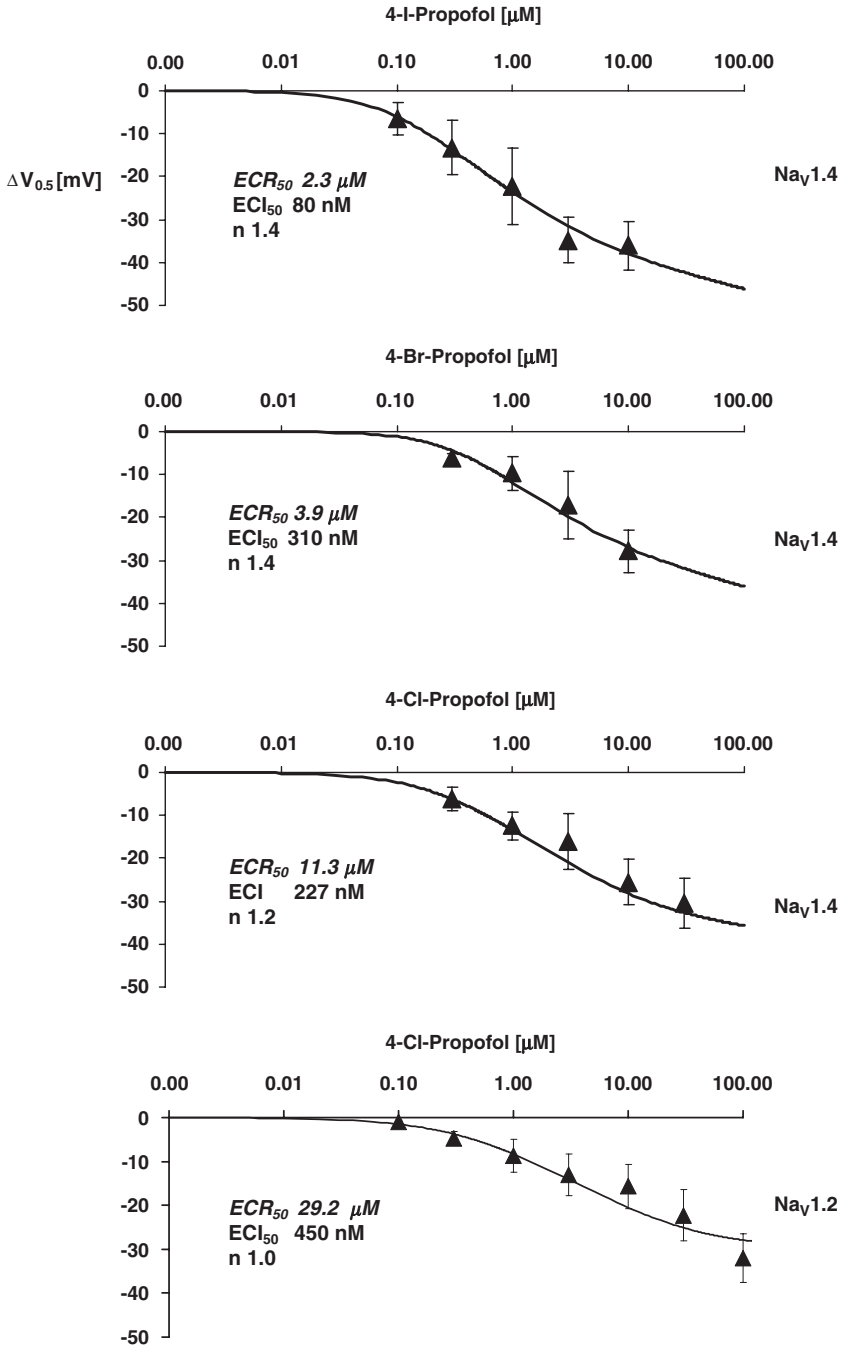

Figure 4 Model-dependent assessment of the affinity to fast-inactivated channels. Concentration dependence of the drug-induced negative shifts in the midpoints ($\Delta V_{0.5}$) of the steady-state availability plots relative to the starting values (from top to bottom) for 4-iodo, 4-bromo- and 4-chloropropofol in $Na_V1.4$, and for 4-chloropropofol in $Na_V1.2$, respectively. Each symbol represents the mean value derived from at least four different experiments each, error bars are standard deviations. The solid line is a least-squares fit of Equation 3 (Materials and methods section) to the averaged data. Parameters inserted as constant factors into the equation are printed in italics, the slope factor *k* was derived from Boltzmann fits to the control data and the ECR_{50} is derived from concentration–response curves at −150 mV. The estimated concentrations for half-maximum effect on inactivated channels (ECI_{50}) derived from that fit were 81, 312 and 227 nM for 4-iodopropofol, 4-bromopropofol and 4-chloropropofol in $Na_V1.4$, respectively, and 450 nM for 4-chloropropofol in $Na_V1.2$. The Hill coefficients for inactivated state binding ranged between 1.4 and 1.0.

muscle sodium channels in the single-digit μM range at a potential close to the normal resting potential (−70 mV) and in the nM range when channels are in fast-inactivated channel states. All propofol analogues showed a marked increase in affinity at depolarized membrane potentials, revealed by a 20- to 40-fold lower half-maximum effect concentration in inactivated channels compared with resting channels. This strong voltage dependency of the block seen with all halogenated propofol analogues is a prominent feature of a local anaesthetic-like action, in general (Bean

et al., 1983; Fan *et al*., 1996; Balser *et al*., 1996b; Scheuer, 1999). The difference in potency between inactivated and resting channels is even greater for the propofol analogues than for lidocaine. For lidocaine, we have previously found an ECI_{50} of 67 μM and an ECR_{50} of 417 μM applying the same modified model to assess inactivated state binding used in this study (Leuwer *et al*., 2004). Tighter binding to inactivated channels and stabilization of inactivated states is a common principle by which local anaesthetic-like compounds target membranes with altered functional expression of voltage-gated sodium channels at doses far below those that block normal nerve and muscle impulse propagation (Rogawski and Löscher, 2004; Bräu *et al*., 2001; Jurkat-Rott *et al*., 2002; Lai *et al*., 2004; Amir *et al*., 2006); Wang *et al*., 2004). It is noteworthy that halogenated propofol analogues dissociate much faster from inactivated channel states than lidocaine. In the presence of lidocaine, the time constants of recovery are prolonged by around 100-fold compared with normal recovery from inactivation resulting in a pronounced use-dependent block even at low stimulating frequencies (Bean *et al*., 1983; Vedantham and Cannon, 1999). Halogenated propofol analogues stabilize inactivation revealed by a moderate (around 10-fold) prolongation of recovery from fast inactivation, which results in an accumulation of block during repetitive depolarizations only when applied at high frequencies (⩾100 Hz). Both inflammatory and neuropathic pain conditions and sodium channel myopathies are associated with increased responsiveness to a spectrum of stimuli or spontaneous firing due to altered function or expression pattern of sodium channels (Waxman and Hains, 2006; Jurkat-Rott *et al*., 2002; Amir *et al*., 2006). High-frequency electrical discharges that may result from ectopic activity at the site of a nerve injury or infarcted area are especially sensitive to lidocaine-like local anaesthetic and anti-epileptic drugs. For example, systemic lidocaine silences ectopic discharge patterns at the site of an experimental nerve injury and in axotomized dorsal root ganglion cells at doses that leave normal impulse propagation unaffected (Devor *et al*., 1992). The strong dependence of blocking potency on the kinetic state of the channel along with rapid drug dissociation from inactivated channels hypothetically makes the halogenated propofol analogues useful candidates for selectively suppressing pathological ectopic discharges in damaged tissues with fewer systemic side effects. This approach might be an interesting perspective in the treatment of certain pain conditions, myotonias or cardiac arrhythmias arising from ectopic discharge patterns in damaged tissues.

As has been shown earlier using the example of phenol and aniline (Zamponi and French, 1993), the interaction with voltage-operated sodium channels does not necessarily require the unsubstituted phenolic hydroxyl group. In

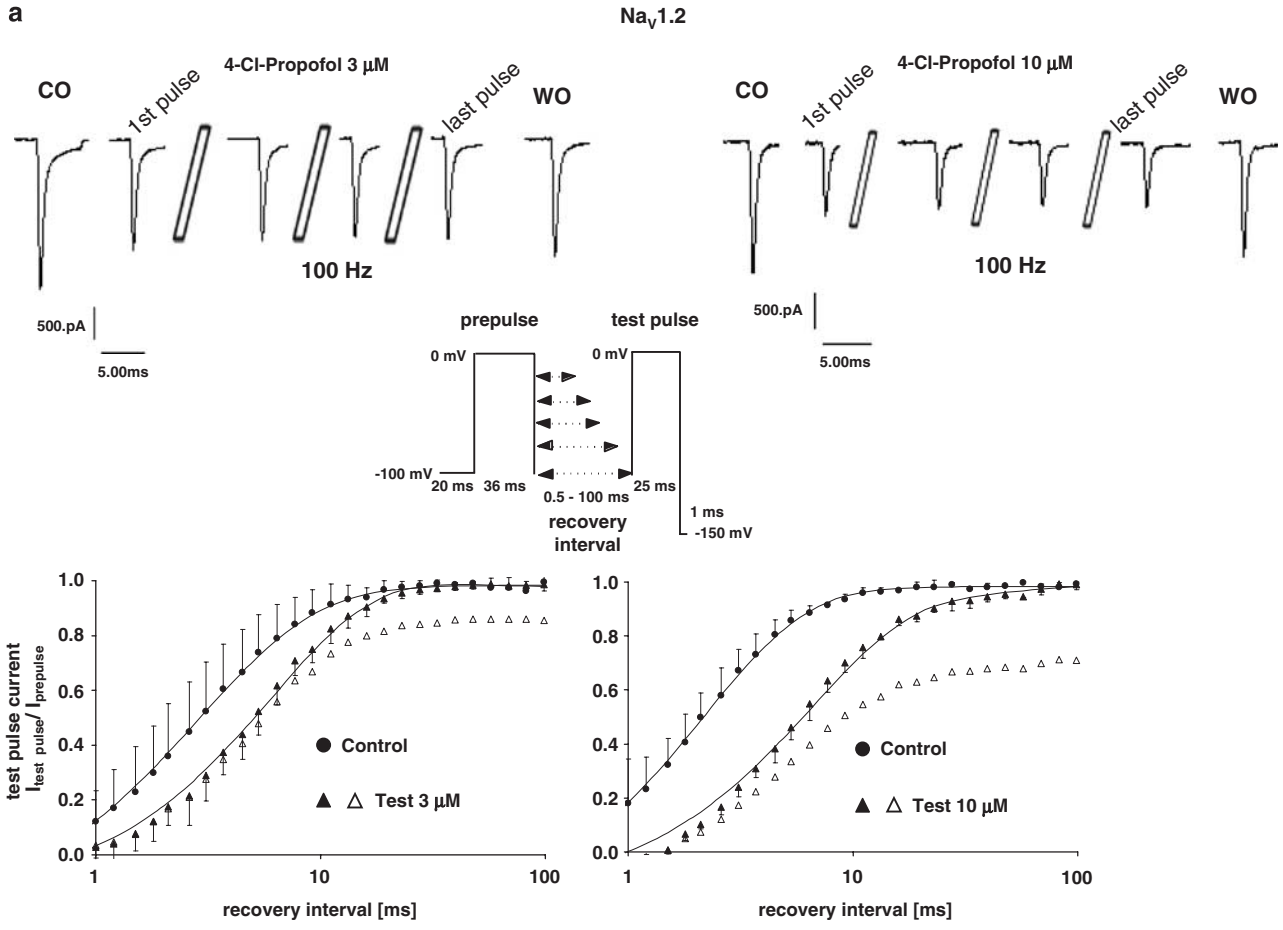

Figure 5 Continued.

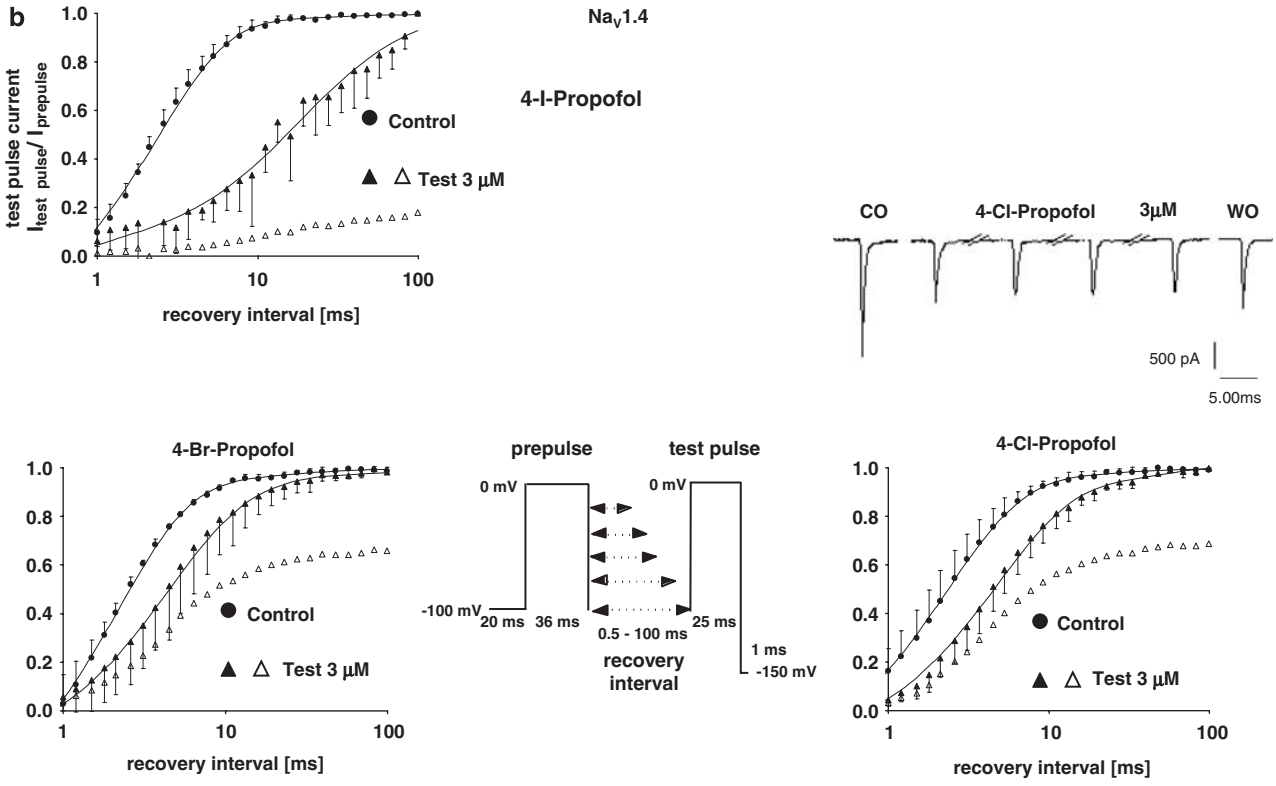

Figure 5 Prolongation of the time course of recovery from fast inactivation and use-dependent block induced by 4-chloropropofol in $Na_V1.2$ (**a**) and by 4-iodo-, 4-bromo- and 4-chloropropofol in $Na_V1.4$ (**b**). (**a**) Upper panel, use-dependent block: representative current traces showing the first trace (control and washout) and the first and the last three traces in the presence of 4-chloropropofol out of a series of 10 depolarizations from −100 to 0 mV applied at 100 Hz. The current traces show a moderate use dependence of the effect of 4-chloropropofol revealed by an increase in the blocking effect from the first pulse to the last pulse of approximately 10% in 10 µM 4-chloropropofol (right row of traces). Lower panel: prolongation of recovery from sodium channel inactivation induced by 4-chloropropofol assessed by a two-pulse protocol at −100 mV membrane potential in $Na_V1.2$ in the controls and in the presence of either 3 µM (left diagram) or 10 µM (right diagram) 4-chloropropofol. The diagrams show the mean fractional current after recovery (ordinate) from five experiments each, plotted against the recovery time interval between inactivating prepulse and test pulse (abscissa) on a logarithmic scale. Error bars are standard deviations. Filled triangles represent the recovered current in the presence of drug normalized to the prepulse current in the presence of drug; empty triangles represent the recovered current in the presence of drug normalized to the prepulse current in the controls. Solid lines are exponential fits (Equation 4) to the data yielding the respective time constants of recovery τ_{rec}. 4-Chloropropofol induces a prolonged recovery from inactivation which shows concentration dependence. (**b**) Prolongation of recovery from sodium channel inactivation induced by 3 µM concentrations of 4-iodopropofol (top), 4-bromopropofol (bottom, left) and 4-chloropropofol (bottom, right) at −100 mV membrane potential in $Na_V1.4$. The diagrams show the mean fractional current after recovery (ordinate) from 4–5 experiments each, plotted against the recovery time interval between inactivating prepulse and test pulse (abscissa) on a logarithmic scale. Error bars are standard deviations. Filled triangles represent the recovered current in the presence of drug normalized to the prepulse current in the presence of drug, empty triangles represent the recovered current in the presence of drug normalized to the prepulse current in the controls. Solid lines are exponential fits (Equation 4) to the data yielding the respective time constants of recovery τ_{rec}. All compounds prolong recovery from inactivation in $Na_V1.4$. The insets show representative current traces showing the first trace out of a series of 10 in the absence of drug (control and washout) and the first and the last three traces in the presence of 3 µM 4-chloropropofol. The current traces show a moderate use dependence of the blocking effect of 4-chloropropofol during 100 Hz trains revealed by an additional fall in the last pulse relative to the first pulse in the presence of drug of around 15%.

contrast, the substitution of this functionally active group at the benzene ring has important implications for additional effects of the compounds on different ion channels and receptors. Although local anaesthetics and phenol derivatives both block voltage-operated sodium channels, they differ profoundly in their effects on the major receptor for inhibitory neurotransmission in the mammalian brain, the γ-aminobutyric acid ($GABA_A$) receptor. Local anaesthetics like lidocaine, bupivacaine, procaine, benzocaine and cocaine inhibit GABA-induced currents, a mechanism that might underlie their CNS toxicity and thus determine their side-effect profile (Hara *et al*., 1995; Ye *et al*., 1997; Sugimoto *et al*., 2000).

In contrast, 2,6-dimethylphenol and a series of other phenol derivatives, in particular propofol, potentiate currents elicited by low concentrations of GABA and activate Cl^- currents through $GABA_A$ receptors in the absence of GABA (Trapani *et al*., 1998; Krasowski *et al*., 2001; Mohammadi *et al*., 2001). This effect, which is supposed to cause the sedative properties of phenol derivatives *in vivo* (Krasowski *et al*., 2001; Jurd *et al*., 2003), strongly depends on the hydrogen bond donor/acceptor properties of the phenolic hydroxyl group (Trapani *et al*., 1998). Consequently, it is reasonable to assume that local anaesthetics based on phenol derivatives would potentially lack some of the side-effect profile of lidocaine-like local anaesthetics. However,

one major concern is that, in principle, all phenol derivatives with GABA agonist properties might induce anaesthesia when injected intravenously in very high concentrations. A previous study showed that 4-iodopropofol, in contrast to propofol, did not produce general anaesthesia following intraperitoneal injection, but possessed marked anti-seizure and anti-conflict activity in rats (Sanna *et al*., 1999). A subsequent study partly challenged the hypothesis of a distinct pharmacological profile of 4-iodopropofol, showing that 4-iodopropofol produced anaesthesia in rats following intravenous administration of very high doses (Lingamaneni *et al*., 2001). The molar potency of 4-iodopropofol to produce anaesthesia after intravenous injection was sixfold lower than that of propofol, and the fact that all animals survived these large doses of 4-iodopropofol suggests a broad therapeutic range with regard to cardiovascular collapse. Furthermore, the observation of anti-convulsant and anti-conflict effects of 4-iodopropofol—accompanied by inhibition of hippocampal acetylcholine release measured by microdialysis *in vivo* (Sanna *et al*., 1999)—after intraperitoneal injection in the absence of general anaesthesia strongly suggests that these effects are extremely sensitive to low, sub-anaesthetic concentrations of 4-iodopropofol. The next logical steps in the development of these compounds will have to include *in vivo* studies in animals assessing the ability of the compounds to produce regional nerve block, their anti-nociceptive and anti-arrhythmic properties and their toxicity profile.

In summary, our study shows that halogenated propofol analogues constitute a novel class of high-affinity sodium channel-blocking drugs. Of particular importance is the fact that channel inactivation substantially increases binding affinity of halogenated propofols as revealed by half-maximum effect concentrations in the nM range. This distinct pharmacological profile *in vitro* might translate into a distinct advantageous pharmacological profile *in vivo* with an emphasis on local anaesthetic, analgesic, anti-spasmodic, anti-arrhythmic and anti-convulsant effects. Owing to the fact that halogenated propofol analogues in low concentrations certainly do not exhibit $GABA_A$ receptor antagonistic properties, they may help to address a long-standing clinically important problem: the pro-convulsive side effects of lidocaine-like local anaesthetics.

Acknowledgements

We are indebted to Professor Frank Lehmann-Horn, Ulm, Germany, for providing us with transfected cells, to Jobst Kilian and Andreas Niesel, Department of Neurology, Hannover, Germany, for technical support and to Irene Wircins, Department of Anesthesiology, Hannover, Germany, for taking care of the cell culture.

Conflict of interest

This work was supported by institutional funding and by an unrestricted grant from B Braun, Melsungen, Germany. Some of the effects of halogenated propofols presented here are covered by a patent (No. 01996375.0-2112-EPO113082). This patent was granted to B Braun in December 2005. G Haeseler and M Leuwer are named inventors. M. Leuwer is a paid consultant to B. Braun.

References

Alexander SPH, Mathie A, Peters JA (2008). Guide to receptors and channels (GRAC). 3rd edn *Br J Pharmacol* **153**: S1–S209.

Amir R, Argoff CE, Bennett GJ, Cummins TR, Durieux ME, Gerner P *et al*. (2006). The role of sodium channels in chronic inflammatory and neuropathic pain. *J Pain* **7**: S1–S29.

Balser JR, Bradley Nuss H, Chiamvimonvat N, Pérez-Garcìa MT, Marban E, Tomaselli GF (1996a). External pore residue mediates slow inactivation in μ 1 rat skeletal muscle sodium channels. *J Physiol* **494**: 431–442.

Balser JR, Bradley Nuss H, Romashko DN, Marban E, Tomaselli GF (1996b). Functional consequences of lidocaine binding to slow-inactivated sodium channels. *J Gen Physiol* **107**: 643–658.

Bean BP, Cohen CJ, Tsien RW (1983). Lidocaine block of cardiac sodium channels. *J Gen Physiol* **81**: 613–642.

Bracken N, Dubuis E, Haeseler G, Leuwer M, Hart G, Hussain M (2006). Halogenated phenol derivatives inhibit the fast sodium current (I_{Na}) with differential potency in rat ventricular myocytes. *J Mol Cell Cardiol* **40**: 985.

Bräu ME, Dreimann M, Olschewski A, Vogel W, Hempelmann G (2001). Effect of drugs used for neuropathic pain management on tetrodotoxin-resistant N^+ currents in rat sensory neurons. *Anesthesiology* **94**: 137–144.

Chahine M, Bennett P, George A, Horn R (1994). Functional expression and properties of the human skeletal muscle sodium channel. *Pflügers Arch* **427**: 136–142.

Devor M, Wall PD, Catalan N (1992). Systemic lidocaine silences ectopic neuroma and DRG discharge without blocking nerve conduction. *Pain* **48**: 261–268.

Fan Z, George AL, Kyle JW, Makielski JC (1996). Two human paramyotonia congenita mutations have opposite effects on lidocaine block of Na+ channels expressed in a mammalian cell line. *J Physiol* **496**: 275–286.

Godwin SA, Cox JR, Wright SN (2005). Modeling of benzocaine analog interactions with the D4S6 segment of NaV1.4 voltage-gated sodium channels. *Biophys Chem* **113**: 1–7.

Graham FL, Van der Eb AJ (1973). A new technique for the assay of infectivity of human adenovirus 5 DNA. *Virology* **52**: 456–467.

Haeseler G, Bufler J, Merken S, Dengler R, Aronson J, Leuwer M (2002). Block of voltage-operated sodium channels by 2,6-dimethylphenol, a structural analogue of lidocaine's aromatic tail. *Br J Pharmacol* **137**: 285–293.

Haeseler G, Leuwer M (2003). High-affinity block of voltage-operated rat IIA neuronal sodium channels by 2,6 di-*tert*-butylphenol, a propofol analogue. *Eur J Anaesthesiol* **20**: 220–224.

Haeseler G, Petzold J, Hecker H, Würz A, Dengler R, Piepenbrock S *et al*. (2000). Succinylcholine metabolite succinic acid alters steady-state activation in muscle sodium channels. *Anesthesiology* **92**: 1385–1392.

Haeseler G, Piepenbrink A, Bufler J, Dengler R, Aronson JK, Piepenbrock S *et al*. (2001a). Structural requirements for voltage-dependent block of muscle sodium channels by phenol derivatives. *Br J Pharmacol* **132**: 1916–1924.

Haeseler G, Störmer M, Bufler J, Dengler R, Hecker H, Piepenbrock S *et al*. (2001b). Propofol blocks skeletal muscle sodium channels in a voltage-dependent manner. *Anesth Analg* **92**: 1192–1198.

Hamill OP, Marty A, Neher E, Sakmann B, Sigworth FJ (1981). Improved patch-clamp techniques for high-resolution current recording from cells and cell-free membrane patches. *Pflügers Arch* **391**: 85–100.

Hara M, Kai Y, Ikemoto Y (1995). Local anesthetics reduce the inhibitory neurotransmitter-induced current in dissociated hippocampal neurons of the rat. *Eur J Pharmacol* **283**: 83–89.

Hille B (1992). Mechanisms of block. In: Hille B (ed). *Ionic Channels of Excitable Membranes* 2nd edn. Sinauer Associates: Sunderland, MA, pp 390–422.

Hodgkin AL, Horowicz P (1959). The influence of potassium and chloride ions on the membrane potential of single muscle fibres. *J Physiol* **148**: 127–160.

Jurd R, Arras M, Lambert S, Drexler B, Siegwart R, Crestani F *et al*. (2003). General anesthetic actions *in vivo* strongly attenuated by a point mutation in the $GABA_A$ receptor β3 subunit. *FASEB J* **17**: 250–252.

Jurkat-Rott K, Lerche H, Lehmann-Horn F (2002). Skeletal muscle channelopathies. *J Neurol* **249**: 1493–1502.

Krasowski MD, Jenkins A, Flood P, Kung AY, Hopfinger AJ, Harrison NL (2001). General anesthetic potencies of a series of propofol analogs correlate with potency for potentiation of γ-aminobutyric acid (GABA) current at the $GABA_A$ receptor but not with lipid solubility. *J Pharmacol Exp Therapeut* **297**: 338–351.

Lai J, Porreca F, Hunter JC, Gold MS (2004). Voltage-gated sodium channels and hyperalgesia. *Annu Rev Pharmacol Toxicol* **44**: 371–397.

Leuwer M, Haeseler G, Hecker H, Bufler J, Dengler R, Aronson J (2004). An improved model for the binding of lidocaine and structurally related local anaesthetics to depolarized states of voltage-operated sodium channels. *Br J Pharmacol* **141**: 47–54.

Lingamaneni R, Krasowski MD, Jenkins A, Truong T, Giunta AL, Blackbeer J *et al*. (2001). Anesthetic properties of 4-iodopropofol. *Anesthesiology* **94**: 1050–1057.

Mitrovic N, George AL, Heine R, Wagner S, Pika U, Hartlaub U *et al*. (1994). K+-aggravated myotonia: destabilization of the inactivated state of the human muscle sodium channel by the V1589M mutation. *J Physiol* **478**: 395–402.

Mohammadi B, Haeseler G, Leuwer M, Dengler R, Krampfl K, Bufler J (2001). Structural requirements of phenol derivatives for direct activation of chloride currents via $GABA_A$- receptors. *Eur J Pharmacol* **421**: 85–91.

Rogawski MA, Löscher W (2004). The neurobiology of antiepileptic drugs for the treatment of nonepileptic conditions. *Nature Med* **10**: 685–692.

Sanna E, Motzo C, Usala M, Serra M, Dazzi L, Maciocco E *et al*. (1999). Characterization of the electrophysiological and pharmacological effects of 4-iodo-2,6-diisopropylphenol, a propofol analogue devoid of sedative-anaesthetic properties. *Br J Pharmacol* **126**: 1444–1454.

Sarkar SN, Adhikari A, Sikdar SK (1995). Kinetic characterization of rat brain type IIA sodium channel α-subunit stably expressed in a somatic cell line. *J. Physiol.* **488**: 633–645.

Scheuer T (1999). A revised view of local anesthetic action: what channel state is really stabilized? *J Gen Physiol* **113**: 3–6.

Sugimoto M, Uchida I, Fukami S, Takenoshita M, Mashimo T, Yoshiya I (2000). The α and γsubunit-dependent effects of local anaesthetics on recombinant $GABA_A$ receptors. *Eur J Pharmacol* **401**: 329–337.

Tikhonov DB, Bruhova I, Zhorov BS (2006). Atomic determinants of state-dependent block of sodium channels by charged local anesthetics and benzocaine. *FEBS Lett* **580**: 6027–6032.

Trapani G, Latrofa A, Franco M, Altomare C, Sanna E, Usala M *et al*. (1998). Propofol analogues. Synthesis, relationships between structure and affinity at $GABA_A$ receptor in rat brain, and differential electrophysiologial profile at recombinant human $GABA_A$ receptors. *J Med Chem* **41**: 1846–1854.

Vedantham V, Cannon SC (1999). The position of the fast-inactivation gate during lidocaine block of voltage-gated Na+ channels. *J Gen Physiol* **113**: 7–16.

Wang DW, George AL, Bennett PB (1996). Comparison of heterologously expressed human cardiac and skeletal muscle sodium channels. *Biophys J* **70**: 238–245.

Wang GK, Russel C, Wang S-Y (2004). State-dependent block of voltage-gated Na+ channels by amitriptyline via the local anesthetic receptor and its implications for neuropathic pain. *Pain* **110**: 166–174.

Waxman SG, Hains BC (2006). Fire and phantoms after spinal cord injury: Na+ channels and central pain. *Trends Neurosci* **29**: 207–215.

Ye JH, Liu PL, Wu WH, McArdle JJ (1997). Cocaine depresses $GABA_A$ current of hippocampal neurons. *Brain Res* **770**: 169–175.

Zamponi GW, French RJ (1993). Dissecting lidocaine action: diethylamide and phenol mimic separate modes of lidocaine block of sodium channels from heart and rat skeletal muscle. *Biophys J* **65**: 2335–2347.

Supplementary Information accompanies the paper on British Journal of Pharmacology website (http://www.nature.com/bjp)